HHS Public Access

Author manuscript

Dev Biol. Author manuscript; available in PMC 2015 April 01.

Published in final edited form as:

Dev Biol. 2015 April 1; 400(1): 139–147. doi:10.1016/j.ydbio.2015.01.023.

Region-specific regulation of cell proliferation by FGF receptor signaling during the Wolffian duct development

Mika Okazawa[a,b,1], **Aki Murashima**[a,1], **Masayo Harada**[c], **Naomi Nakagata**[d], **Masafumi Noguchi**[e], **Mitsuru Morimoto**[e], **Tadashi Kimura**[b], **David M. Ornitz**[f], and **Gen Yamada**[a,*]

[a]Department of Developmental Genetics, Institute of Advanced Medicine, Wakayama Medical University, 811-1 Kimiidera, Wakayama 641-8509, Japan

[b]Department of Obstetrics and Gynecology, Osaka University Graduate School of Medicine, 2-2 Yamadaoka, Suita 565-0871, Osaka, Japan

[c]Department of Clinical Anatomy, Graduate School of Medical and Dental Sciences, Tokyo, Medical and Dental University, 1-5-45 Yushima, Bunkyo-ku 113-8519, Tokyo, Japan

[d]Division of Reproductive Engineering, Center for Animal Resources and Development, Kumamoto University, 2-2-1 Honjo, Kumamoto 860-0811, Japan

[e]Laboratory for Lung Development, RIKEN Center for Developmental Biology, 2-2-3 Minatojima-minamimachi, Chuou-ku, Kobe 650-0047, Hyogo, Japan

[f]Department of Developmental Biology, Washington University School of Medicine, St. Louis, MO 63110, USA

Abstract

The Wolffian duct (WD) is a primordium of the male reproductive tract and kidney collecting duct system. Fibroblast growth factor receptors (FGFRs), members of the receptor tyrosine kinase (RTK) family, are essential for kidney development. Although the functions of FGFR signaling in kidney morphogenesis have been analyzed, their function in WD development has not been comprehensively investigated. Here, we demonstrate that *Fgfr2* is the major *Fgfr* gene expressed throughout the WD epithelia and that it is essential for the maintenance of the WD, specifically in the caudal part of the WD. *Hoxb7-Cre* mediated inactivation of *Fgfr2* in the mouse WD epithelia resulted in the regression of the caudal part of the WD and abnormal male reproductive tract development. Cell proliferation and expression of the downstream target genes of RTK signaling (*Etv4* and *Etv5*) were decreased in the caudal part of the WD epithelia in the mutant embryos. Cranial (rostral) WD formation and ureteric budding were not affected. *Ret*, *Etv4*, and *Etv5* expression were sustained in the ureteric bud of the mutant embryos. Taken together, these data suggest region-specific requirements for FGFR2 signaling in the developing caudal WD epithelia.

*Corresponding author. Fax: +81 73 499 5026., transg8@wakayama-med.ac.jp, genyama77@yahoo.co.jp (G. Yamada).

[1]These authors contributed equally to this work.

Keywords

Fgfr; Ret; Receptor tyrosine kinase; Cell proliferation; Wolffian duct; Ureteric bud

Introduction

The Wolffian duct (WD) is a primordium of the male reproductive tract, which develops into the epididymis, vas deferens, and seminal vesicles. In addition, the WD plays a crucial role in kidney development as the primordium for the ureter and kidney collecting duct system (Bouchard et al., 2002; Saxen, 1987). In mouse embryos, the WD is formed in the anterior intermediate mesoderm at embryonic (E) day 8.5 (E8.5), elongating caudally to reach the cloaca by E9.5 (Atsuta et al., 2013; Davidson, 2009). WD insertion into the cloaca has been reported to be essential for ureter positioning (Chia et al., 2011; Weiss et al., 2014). Three successive kidneys develop along the WD in an anterior–posterior manner: the pronephros, mesonephros, and metanephros (Capel, 2000). The pronephros is formed at the most anterior level of the WD at E8.5, and degenerates by E9.5 (Dressler, 2006). The mesonephros is subsequently formed posterior to the pronephros. The cranial part of the mesonephric mesenchyme differentiates into the mesonephric tubules (MTs) (Dressler, 2006). Degeneration of the mesonephric mesenchyme begins from caudal at E10.5 and extends cranially (Hoshi et al., 2012). At the same time, in the caudal end of the mesonephros, the WD develops a multilayered, “pseudostratified epithelia”, forming the ureteric bud (UB) (Chi et al., 2009). The metanephros, which is the definitive kidney in mammals, begins to form from the UB and adjacent metanephric mesenchyme (MM) (Yu et al., 2004). Malformation of the WD in the caudal mesonephros, in addition to the UB, often results in the congenital anomalies in human, such as duplex ureter and absence of the vas deferens. The characterization of the nephrogenic regions, especially the caudal mesonephros, has just started to be understood for their susceptibility to such developmental abnormality (Hoshi et al., 2012; Murashima et al., 2014; Nishita et al., 2014).

The reciprocal interaction between the WD epithelia and adjacent nephrogenic mesenchyme is essential for the morphogenesis of all kidney structures (Batourina et al., 2001). In such interactions, growth factor signaling, including Glial cell line-derived neurotrophic factor (Gdnf), Wnt, and Fibroblast growth factor (Fgf), are well characterized signaling pathways. Dysregulation of these signaling pathways often causes ectopic UB formation, mostly in the caudal part of the mesonephros (Basson et al., 2005; Brophy et al., 2001; Grieshammer et al., 2004; Kume et al., 2000; Mendelsohn, 2009; Michos et al., 2004; Nishita et al., 2014; Shakya et al., 2005).

Receptor tyrosine kinase (RTK) signaling is a key requirement for the development of many organs. It regulates cellular processes including proliferation, survival, differentiation, and migration (Schlessinger, 2000). Binding of ligands to their RTKs activates several intracellular pathways such as phosphoinositide 3-kinase (PI3K)/AKT, mitogen-activated protein kinase (MAPK), and phospholipase C-gamma (PLC-gamma) (Song et al., 2011). Several RTKs such as Rearranged during transfection (RET) and Fgf receptor (FGFR) play an essential role in vertebrae embryonic development, especially in mammalian kidney

development (Bates, 2011; Benazeraf and Pourquie, 2013; Costantini and Shakya, 2006; Moore et al., 1996; Pichel et al., 1996; Sainio et al., 1997; Sanchez et al., 1996; Schuchardt et al., 1994).

There are four FGFRs that interact with 18 known FGF ligands in mammals (Beenken and Mohammadi, 2009; Ornitz and Itoh, 2001). The expression of *Fgfr1* and *Fgfr2* is detected in the metanephros and in the cranial part of the mesonephros (Cancilla et al., 1999; Dudley et al., 1999; Kitagaki et al., 2011; Orr-Urtreger et al., 1991; Peters et al., 1992; Poladia et al., 2006; Zhao, 2004). In contrast, *Fgfr3* and *Fgfr4* are not detected in the mesonephros (Kitagaki et al., 2011). Conditional knockout (KO) approaches in mice have revealed that *Fgfr1* and *Fgfr2* in the kidney mesenchyme are crucial for early MM formation and UB induction (Hains et al., 2008; Poladia et al., 2006; Walker et al., 2013). On the other hand, epithelial FGFR signaling regulates the branching morphogenesis of the metanephric kidney, possessing minor functions on initial UB formation (Zhao, 2004). Recent studies indicate that FGFR signaling may compensate loss of GDNF/RET signaling, which is the most essential RTK signaling for the ureteric budding (Maeshima et al., 2007; Michos et al., 2010; Tee et al., 2013). Although the functions of FGF signaling in metanephric kidney morphogenesis have been analyzed, its function in WD development has not been well described. In addition, the possible compensation between different RTKs in the WD has not been investigated.

In this study, we examined the roles of FGFR signaling in the WD using mouse genetic models. WD-specific inactivation of *Fgfr2* revealed a developmental region-specific function for FGFR2 on regulation of cell proliferation.

Materials and methods

Mice

The mouse strains used herein were *Fgfr1*^{flox} (Zhao et al., 2007), *Fgfr2*^{flox} (Yu et al., 2003), *Hoxb7-Cre* (Yu et al., 2002), *ROSA26-LacZ* (Soriano, 1999), *ROSA26-YFP* (Srinivas et al., 2001), *Ret-GFP* (Enomoto et al., 2001) and ICR (CLEA, Tokyo, Japan). *Hoxb7-Cre* mice and *ROSA26-YFP* mice were obtained from Jackson Laboratory. *Fgfr2*-null alleles were generated by crossing *Fgfr2*^{flox} mice to *CAGGS-Cre* mice (Araki et al., 1997), which express Cre recombinase in the germline. All experimental procedures and protocols were approved by the Animal Research Committee of the Wakayama Medical University and Kumamoto University. Embryos for each experiment were collected from at least three pregnant females. Noon on the day when a vaginal plug was detected was designated as E0.5. Embryos used for analyses at E10.5 were not identified their gender. Male embryos were used for the analyses at E12.5 and later.

Histology and immunohistochemistry

Tissues were fixed in 4% paraformaldehyde, dehydrated, embedded in paraffin, and sectioned. Hematoxylin and eosin (HE) staining was performed by standard procedures as previously described (Haraguchi et al., 2000). For immunohistochemistry, deparaffinized sections were treated for antigen retrieval (autoclave 121 °C for 1 min in 10 mM citrate

buffer at pH 6.0) and incubated with 3% H_2O_2 in methanol for 10 min to inactivate endogenous peroxidase before 1 h incubation with a blocking solution (1.5% fetal bovine serum (FBS) in PBS). Anti-cleaved caspase-3 polyclonal antibody (Cell Signaling Technology, Danvers, MA, 1:1000), anti-ZO-1 polyclonal antibody (Invitrogen, Carlsbad, CA, 1:200), anti-laminin polyclonal antibody (Sigma-Aldrich, St. Louis, MO, 1:100), or anti-E-cadherin monoclonal antibody (BD Biosciences, San Jose, CA, 1:400) in PBS solution was added to the slides and incubated for 1 h at room temperature. Negative controls were obtained by excluding the primary antibodies. After washing with PBS, the sections were stained with the Vectastain ABC Kit (Vector Laboratories, Burlingame, CA) or incubated with Alexa 546/488-labeled goat anti-rabbit/mouse IgG (Life Technologies, Grand Island, NY) or horseradish peroxidase-labeled rabbit anti-goat IgG (Zymed, South San Francisco, CA) for 1 h at room temperature. Where indicated, the sections were subsequently incubated with 3, 3-diaminobenzidine tetrahydrochloride (DAB) containing H_2O_2. Sections were counterstained by Hoechst 33342 (Sigma-Aldrich), Hematoxylin (Wako, Osaka, Japan), or Methyl Green (Sigma-Aldrich).

Cell proliferation assay

Pregnant females were injected intraperitoneally with 25 mg 5-ethynyl-2′-deoxyuridine (EdU; Invitrogen) per 1 kg body weight. One hour after injection, embryos were collected. Embryos were fixed and processed for paraffin-embedding as described above. Serial horizontal sections (6 μm/section) were made from the cranial end to the caudal end of the WD. EdU-labeled cells were stained using the Click-iT EdU Alexa Fluor 555 Imaging Kit (Invitrogen) according to the supplier's instructions. The total cell number (stained by Hoechst) and the total number of EdU-positive cells were counted for each epithelial portion. The percentage proliferation was calculated as the fraction of EdU-positive cells over the total number of nuclei. Statistical analysis was performed using the Mann–Whitney test ($P<0.05$ was considered significant).

Whole-mount and section RNA in situ hybridization for gene expression

Whole-mount and section *in situ* hybridization was performed using digoxigenin-labeled probes as previously described (Haraguchi et al., 2000). Probes for the following genes were used: *Pax2* (Dressler et al., 1990), *Fgfr1* (kindly provided by Dr. J. Partanen), *Fgfr2* (Ozawa et al., 1996), *Etv4* (provided by Dr. D. M. Ornitz), *Etv5* (provided by Dr. D. M. Ornitz), *Ret* (Nishinakamura et al., 2001), *Gdnf* (Nishinakamura et al., 2001), and *Fgf10* (kindly provided by Dr. H. Ohuchi and Dr. N. Itoh). For the confirmation of the *Fgfr2* mutation, a probe that does not recognize the mutated allele was used (Yu et al., 2003).

Results

Fgfr2 is the major Fgfr gene expressed in the WD epithelia

Although *Fgfr* expression has been partially reported, their expression in the mesonephros has been poorly described. To identify patterns of *Fgfr* expression in the WD, whole-mount RNA *in situ* hybridization was performed at E10.5. *Fgfr1* and *Fgfr2* were expressed throughout the mesonephros of wild-type embryos at E10.5 (Fig. 1A and E, arrow). *Fgfr1* expression was more prominent in the MTs (Fig. 1A and B, arrowheads) and mesenchyme

(Fig. 1B–D) than that in the epithelia of the WD (Fig. 1B–D, dashed line, indicated in Fig. 1I). In contrast, *Fgfr2* expression was more prominent in the epithelia of the WD (Fig. 1F–H, dashed line, indicated in Fig. 1I) compared to the MTs (Fig. 1E and F, arrowheads) and mesenchyme (Fig. 1F–H). *Fgfr2* expression was also observed in the WD epithelia locating near the cloaca (Fig. 1J, dashed line).

WD-specific inactivation of Fgfr2 results in WD regression in the caudal mesonephros

Cre activity driven by the *Hoxb7* promoter was analyzed by crossing *Hoxb7-Cre* mice with the *ROSA26-LacZ* reporter strain and embryos were analyzed for β-galactosidase (βgal) enzyme activity. βgal-positive cells were located throughout the WD epithelia in *Hoxb7-Cre; ROSA26*$^{LacZ/+}$ embryos at E10.5 and E9.5 (Supplemental Fig. S1A–C) (Kobayashi et al., 2005; Mugford et al., 2008; Yu et al., 2002). Most of the epithelial cells were βgal-positive in the WD, and a few βgal-negative cells were observed in the cranial part (Supplemental Fig. S1A, arrow). A small number of βgal-positive cells were observed in MTs (Supplemental Fig. S1A, arrowhead). The percentage of βgal-positive cells in each region of the WD epithelia of *Hoxb7-Cre; ROSA26*$^{LacZ/+}$ embryos at E10.5 was shown in Supplemental Fig. S1 (*n*=3).

To examine the roles of FGFR2 signaling during WD development, *Hoxb7-Cre; Fgfr2*$^{+/-}$ male mice were crossed with *Fgfr1*$^{flox/flox}$; *Fgfr2*$^{flox/flox}$ female mice to get *Hoxb7-Cre; Fgfr1*$^{flox/+}$; *Fgfr2*$^{flox/-}$ embryos. Hereafter, we refer to *Hoxb7-Cre; Fgfr1*$^{flox/+}$; *Fgfr2*$^{flox/-}$ mice as WD-specific *Fgfr2*-inactivation mice (*Fgfr2*$^{WD\ flox/-}$). Control mice are either heterozygous for the *Fgfr2* floxed allele (*Hoxb7-Cre; Fgfr1*$^{flox/+}$; *Fgfr2*$^{flox/+}$) or lack the *Hoxb7-Cre* transgenic allele.

Inactivation of *Fgfr2* in the WD of *Fgfr2*$^{WD\ flox/-}$ embryos was confirmed by whole-mount RNA *in situ* hybridization. *Fgfr2* was expressed in the WD and MTs in the control embryos at E10.5, while its expression was reduced in *Fgfr2*$^{WD\ flox/-}$ embryos compared to the controls at E10.5 (Fig. 2A and A′, black arrow and arrowheads). To examine the development of WD structure in *Fgfr2*$^{WD\ flox/-}$ mice, whole-mount RNA *in situ* hybridization for *Pax2* was performed. *Pax2* expression was observed in the WD, MTs, and condensed mesenchyme in both control and *Fgfr2*$^{WD\ flox/-}$ embryos at E10.5 (Fig. 2B and B′, black arrow, black arrowheads, and white arrowheads). The MTs were formed along the cranial WD (Fig. 2B and B′, black arrowheads) and the UB invaginated dorsally (Fig. 2B and B′, yellow arrow), showing no significant differences between the control and *Fgfr2*$^{WD\ flox/-}$ embryos. Histological analysis showed a well-established epithelial structure in the cranial part of the WD in both control and *Fgfr2*$^{WD\ flox/-}$ embryos at E10.5 (Fig. 2E and E′, black arrow, indicated in Fig. 2S). In the caudal part, no significant differences were observed in the size of the WD between the control and some *Fgfr2*$^{WD\ flox/-}$ embryos (3 out of total 7 samples), whereas a hypoplastic WD of the caudal mesonephros was observed in other *Fgfr2*$^{WD\ flox/-}$ embryos (4 out of total 7 samples; Fig. 2F and F′, black arrow, also indicated in Fig. 2S). The ductal epithelia reached the cloacal epithelia in both control and *Fgfr2*$^{WD\ flox/-}$ embryos at E10.5 (7 out of total 7 samples; Fig. 2L and L′, black arrowheads). The well-differentiated pseudostratified epithelia of the UB were detected even in *Fgfr2*$^{WD\ flox/-}$ embryos with hypoplastic WD of the caudal mesonephros (Fig. 2G and G′,

also indicated in Fig. 2S). These data indicate that the WD is formed in the mutant embryos by E10.5. At E12.5, the WD marked by *Pax2* expression was observed from cranial to caudal of the control embryos (Fig. 2C). In contrast, such *Pax2* expression was disrupted in the WD of the caudal mesonephros of *Fgfr2*$^{WD\ flox/-}$ embryos (Fig. 2C′, red arrow). Histological analysis revealed that the cranial epithelial structure was indistinguishable between the control and *Fgfr2*$^{WD\ flox/-}$ WD (Fig. 2H and H′, indicated in Fig. 2T). In contrast, the WD of the caudal mesonephros showed regressing epithelia in *Fgfr2*$^{WD\ flox/-}$ embryos (a red arrow in Fig. 2I′, also indicated in Fig. 2T; 8 out of total 10 samples in Table 1). Taken together, these results suggest that epithelial FGFR signaling is essential for the maintenance of the WD, especially in the caudal mesonephros. At E16.5, the control embryos possessed well-differentiated WD derivatives, the epididymis and vas deferens, connected to the urogenital sinus (Fig. 2D). *Fgfr2*$^{WD\ flox/-}$ embryos, on the other hand, showed a dilation of the duct in the cranial WD (Fig. 2D, D′, J, and J′, indicated in Fig. 2U; 4 out of total 6 samples in Table 1), and the epithelial structure was not observed in the vas deferens derived from the WD of the caudal mesonephros (Fig. 2K and K′, also indicated in Fig. 2U).

Functional redundancy of *Fgfr1* and *Fgfr2* has been reported in several developmental systems (Hebert, 2003; Paek et al., 2009; White et al., 2006). To examine the function of *Fgfr1* upon inactivation of *Fgfr2* in the WD epithelia, *Hoxb7-Cre; Fgfr1*$^{flox/-}$; *Fgfr2*$^{flox/-}$ (*Fgfr1/2*$^{WD\ flox/-}$) mice were investigated. *Fgfr1/2*$^{WD\ flox/-}$ embryos showed regressing epithelia in the WD of the caudal mesonephros at E12.5 (Fig. 2N, red arrow; 3 out of total 3 samples in Table 1), as observed in *Fgfr2*$^{WD\ flox/-}$ embryos (Fig. 2I′; 8 out of total 10 samples in Table 1). In contrast, the epithelial structure was indistinguishable in the cranial part between the control and *Fgfr1/2*$^{WD\ flox/-}$ WDs (Fig. 2H and M). At E16.5, the gross morphology of *Fgfr1/2*$^{WD\ flox/-}$ embryos showed dilated duct formation in the cranial part, with an obstructed duct in the caudal part at E16.5 (Fig. 2O; 2 out of total 3 samples in Table 1), as observed in *Fgfr2*$^{\mathrm{WD\ flox/-}}$ embryos (Fig. 2D′; 4 out of total 6 samples in Table 1). By the histological analysis of the *Fgfr1/2*$^{WD\ flox/-}$ WD, the presence of epithelia in the cranial part was observed, while the epithelial structure was not evident in the caudal part (data not shown), as observed in *Fgfr2*$^{WD\ flox/-}$ embryos (Fig. 2J′ and K′). *Hoxb7-Cre; Fgfr1*$^{flox/-}$; *Fgfr2*$^{flox/+}$ (*Fgfr1*$^{\mathrm{WD\ flox/-}}$) embryos showed no obvious phenotypes; well-differentiated WDs reached the urogenital sinus as well as the control WD at E16.5 (Fig. 2R, $n = 4$ in Table 1) and at E12.5 (Fig. 2P and Q; n=8 in Table 1). This is consistent with the absence of prominent *Fgfr1* expression in the WD epithelia during WD development (Fig. 1B–D). These results indicate that *Fgfr2* is the dominant FGF receptor for the maintenance of the WD in the caudal mesonephros, and *Fgfr1* may contribute with a small amount of redundancy.

Decreased expression of the downstream target genes of RTK signaling in the WD epithelia of Fgfr2$^{WD\ flox/-}$ embryos

Etv4 and *Etv5* are downstream targets of RTK signaling including FGFR (Brent and Tabin, 2004; Firnberg and Neubüser, 2002; Liu et al., 2003). The expression pattern of *Etv4* and *Etv5* in the WD was examined at the WD of the cranial and caudal mesonephros, and UB (Fig. 3N). Both *Etv4* and *Etv5* were expressed in the WD epithelia, MT, and condensed

nephrogenic mesenchyme of E10.5 control embryos (dashed line, black arrowhead, and white arrowhead in Fig. 3A–C and D–F). Expression of these genes was reduced in the WD epithelia of the cranial and caudal mesonephros of *Fgfr2*$^{WD\ flox/-}$ embryos, compared to control embryos (Fig. 3A, A′, B, B′, D, D′, E and E′, dashed line). The expression of these genes was not significantly different in the MTs (Fig. 3A, A′, D, and D′, black arrowhead) and the condensed mesenchyme (Fig. 3B, B′, E, and E′, white arrowhead) between the control and *Fgfr2*$^{WD\ flox/-}$ embryos. Notably, the expression of *Etv4* and *Etv5* in the epithelia adjacent to the MM (MM side) was retained at the UB level, whereas it was decreased in the epithelia at the opposite side of the MM (coelom side) in *Fgfr2*$^{WD\ flox/-}$ embryos (Fig. 3C, C′, F, and F′, red arrowheads, indicated in Fig. 3O).

In addition to FGFR signaling, GDNF/RET signaling is also essential RTK signaling for UB formation (Cacalano et al., 1998; Enomoto et al., 1998; Moore et al., 1996; Pichel et al., 1996; Sanchez et al., 1996; Schuchardt et al., 1994). Failure of UB formation is the most frequent phenotype associated with *Gdnf* or *Ret* deficiency (Costantini and Shakya, 2006). In control embryos, *Ret* was expressed throughout the WD epithelia (Fig. 3G–I, dashed line; Fig. 3J, black arrow), with the highest level of expression in the UB at E10.5 (Fig. 3I, dashed line; Fig. 3J, yellow arrow). In contrast, Ret expression was reduced in the WD of the cranial and caudal mesonephros, and in the coelom side of the UB of *Fgfr2*$^{WD\ flox/-}$ embryos (Fig. 3G–I and G′–H′, dashed line, red arrowheads; Fig. 3J and J′, black arrow). Ret expression in the MM side of the UB was not affected in *Fgfr2*$^{WD\ flox/-}$ embryos at E10.5 (Fig. 3I′, dashed line; Fig. 3J′, yellow arrow). These results suggest that *Ret* expression may be regulated by *Fgfr2* in the WD epithelia, except in the MM side of the UB. This observation is consistent with the finding that UB outgrowth was unaffected in *Fgfr2*$^{WD\ flox/-}$ embryos until E13.5 (data not shown) (Zhao, 2004).

In the WD, it is reported that chimeric expression of *Ret* in the UB results in epithelial cell rearrangement to exclude the *Ret*-negative cells from the MM side of the UB (Chi et al., 2009). To trace the lineage of cells in which Cre was activated in the *Fgfr2*$^{WD\ flox/-}$ background, we crossed *Hoxb7-Cre; Fgfr2*$^{+/-}$ mice with *Fgfr2*$^{flox/flox}$; *ROSA26*$^{YFP/YFP}$ mice to obtain *Hoxb7-Cre; ROSA26*$^{YFP/+}$; *Fgfr2*$^{flox/-}$ embryos. Recombined cells, marked by GFP, were distributed throughout the WD and displayed no significant differences when compared with *Hoxb7-Cre; ROSA26*$^{LacZ/+}$ embryos at E10.5 (Supplemental Figs. S1 and S2). Uniform distribution of the recombined cells in the UB was observed in *Fgfr2*$^{WD\ flox/-}$ embryos (Supplemental Fig. S2). These results suggest that *Hoxb7-Cre*-mediated *Fgfr2* gene recombination in the WD was introduced ubiquitously and recombined cell-specific epithelial cell rearrangement may not occur in the *Fgfr2*$^{WD\ flox/-}$ WDs. Taken together, these results suggest that FGFR2 signaling is the major RTK signaling pathway in the WD epithelia, but not in the MM side of the UB, at E10.5.

To examine the involvement of GDNF/RET signaling in *Etv* expression in the WD, we analyzed Ret KO mice at E10.5. *Ret* gene mutations lead to renal agenesis and hypoplasia, and ectopic ureter termination (de Graaff et al., 2001; Enomoto et al., 2001; Jain et al., 2006; Schuchardt et al., 1996). Sustained expression of *Etv4* and *Etv5* was observed in all regions of the WD epithelia of *Ret* KO embryos (dashed line in Fig. 3K–M and K′–M′, data not shown). However, reduced phospho-Erk expression was observed in the MM side of the UB

of *Ret* KO embryos at E10.5 (data not shown), which agrees with the previous finding (Chi et al., 2009). These results suggest that the reduced expression of *Etv4* and *Etv5* observed in *Fgfr2*$^{WD\ flox/-}$ embryos is independent of RET-mediated RTK signaling.

FGFR signaling regulates cell proliferation in the WD of the caudal mesonephros and the coelom side of the UB

To identify the mechanism leading to the regression of the WD of the caudal mesonephros in *Fgfr2*$^{WD\ flox/-}$ embryos, cell proliferation was assessed by EdU incorporation at the WD of the cranial and caudal mesonephros, and UB at E10.5 (Fig. 4A–C and A′–C′; indicated in Fig. 4N). In control embryos, the WD of the caudal mesonephros and the UB displayed higher rate of cell proliferation than the cranial part (Fig. 4A–C). The WD of the caudal mesonephros in the *Fgfr2*$^{WD\ flox/-}$ embryos demonstrated significantly reduced epithelial cell proliferation, compared to the control embryos (Fig. 4B, B′, and M). There were no significant differences in cell proliferation in the cranial part and in the MM side of the UB between the control and *Fgfr2*$^{WD\ flox/-}$ WDs (Fig. 4A, A′, C, C′ and M). Fewer proliferating cell nuclei were observed in the coelom side of the UB in *Fgfr2*$^{WD\ flox/-}$ embryos than in the control embryos (Fig. 4C, C′, and M). Apoptosis, indicated by cleaved caspase-3 expression, was also analyzed in control and *Fgfr2*$^{WD\ flox/-}$ embryos. No significant differences in apoptosis were observed between the control and *Fgfr2*$^{WD\ flox/-}$ embryos at E10.5 (Fig. 4D–F and D′–F′, red arrowheads). These results indicate that FGFR signaling regulates cell proliferation in the WD of the caudal mesonephros and in the coelom side of the UB.

To investigate whether loss of epithelial cell polarity contributes to the epithelial regression observed in *Fgfr2*$^{WD\ flox/-}$ WDs, expression patterns of ZO-1 (Fig. 4G–I and G′–I′), E-cadherin, and laminin (Fig. 4J–L and J′–L′) was analyzed. The core tight junction protein, ZO-1, was detected at the apical side of epithelial cells in both control and *Fgfr2*$^{WD\ flox/-}$ WDs (Fig. 4G–I and G′–I′). E-cadherin, an adherence junction protein, and laminin, a basement membrane component, were detected at the apical and lateral side of the cells and at the basement membrane, respectively, in *Fgfr2*$^{WD\ flox/-}$ WDs as well as in control embryos (Fig. 4J–L and J′–L′). These results suggest that polarized epithelia are established and maintained in *Fgfr2*$^{WD\ flox/-}$ WDs.

Region-specific expression of RTK ligands in the mesonephros and metanephros

FGF7 and FGF10 are ligands with high specificity for the FGFR2-IIIb isoform (Ornitz et al., 1996; Zhang et al., 2006). Previous studies have demonstrated that *Fgf7* is not detected in the developing kidney before E14.5 (Finch et al., 1995; Mason et al., 1994). On the other hand, FGF10 is considered the main ligand for FGFR in the WD (Donjacour et al., 2003).

Fgf10 expression was observed in both the MM and the mesenchyme of the coelom side with a pattern showing a higher expression at the UB level that gradually decreases as it proceeds cranially (Fig. 5A and B, Supplemental Fig. S4). *Gdnf*, a ligand for RET signaling, was expressed mainly in the MM of the control embryos (Fig. 5C and D). Localization of *Fgf10* and *Gdnf* expression in the *Fgfr2*$^{WD\ flox/-}$ embryos was essentially similar to that in the control embryos (Fig. 5A–D and A′–D′).

Discussion

WD as a model for ductal formation and its abnormalities

The current study demonstrates that FGFR2 signaling prevents WD regression in the caudal mesonephros, and that loss of FGFR2 in the WD may lead to dilation of the cranial part of the WD. A previous study using FGF10 null mice reported cystic dilation in the epididymis and degeneration of the vas deferens (Donjacour et al., 2003). However, the corresponding mechanisms were not identified. In the current study, we demonstrated that reduced FGF signaling in the WD epithelia results in WD regression in the caudal mesonephros. Luminal fluid from the testis to the WD is essential for further development of the WD into male reproductive tract (Hinton et al., 2000; Shum et al., 2011; Tong et al., 1996). Since fluid secretion commences at approximately E13–14 in mice (Joseph et al., 2009), the obstruction of the WD in the caudal mesonephros in $Fgfr2^{WD\ flox/-}$ embryos may cause accumulation of the fluid, leading to dilation of the cranial part of the WD at E16.5.

Formation of the common nephric duct (CND), the WD which locates caudally to the UB, was observed in both the control and $Fgfr2^{WD\ flox/-}$ embryos at E12.5 (Supplemental Fig. S3A and A′). At E14.5, the CND was eliminated, and the WD and ureter were separated in the control and $Fgfr2^{WD\ flox/-}$ embryos (Supplemental Fig. S3B, B′, C, and C′; the level of B and B′ is more anterior than that of C and C′). Our observation that the WD and the ureter were inserted into the urogenital sinus separately at E14.5 suggests that the dilation of the cranial epididymal duct was a consequence of the obstruction of the duct, not of back-flow of urine. Another potential mechanism underlying such dilation might be the disruption of oriented cell division, as described previously in the kidney of *Fgfr1* and *Fgfr2* double mutant mice (Sims-Lucas et al., 2012).

The WD also grows craniocaudally after reaching the cloaca. Immunohistochemical analysis for ZO-1, E-cadherin, and laminin expressions indicated that the epithelial cells maintained their characteristics in $Fgfr2^{WD\ flox/-}$ WDs at E10.5. Cell proliferation is considered to be the major contributor for WD elongation, and the WD of the caudal mesonephros is the most mitotically active in the WD (Fig. 4A–C) (Dyche, 1979; Joseph et al., 2009; Michael and Davies, 2004). Considering that apoptosis was not increased in $Fgfr2^{WD\ flox/-}$ WDs compared to control WDs at E10.5, it is possible that decreased cell proliferation in the WD of the caudal mesonephros causes the ductal thinning observed in $Fgfr2^{WD\ flox/-}$ embryos at E12.5 and later. The current study suggests that active cell proliferation regulated by FGFR signaling in the WD of the caudal mesonephros is essential to maintain the ductal size and epithelial integrity in the growing duct at a later stage.

RTK signaling via FGFR is required for WD development

The current study demonstrates that WD epithelial cell proliferation is regulated by distinct region-specific FGFR signaling.

The frequency of βgal-negative cells in the cranial WD epithelia of *Hoxb7-Cre;* $ROSA26^{LacZ/+}$ embryos was higher than that in the WD of the caudal mesonephros and UB. It is possible that the sustained epithelial cell proliferation in the cranial part of mutant WDs might be due to lower activity of *Hoxb7-Cre* in the cranial WD epithelia. However,

significant reduction of active RTK signaling, indicated by *Etv4* and *Etv5* expression, was observed in the cranial part of $Fgfr2^{WD\ flox/-}$ WDs compared to control WDs. These results suggest that RTK signaling is sufficiently reduced in the cranial part of $Fgfr2^{WD\ flox/-}$ WDs. Taken together, RTK signaling through *Etv4* and *Etv5* may possess less contribution to epithelial cell proliferation in the cranial WD. *Fgf8* is expressed in MTs at E10.5 and its mesoderm-specific conditional KO mice display degeneration in the cranial part of the WD and missing cranial MTs (Kitagaki et al., 2011). Moreover, mesoderm-specific conditional KO mice for *Fgfr1* and *Fgfr2* show loss of the WD and MTs (Kitagaki et al., 2011). These observations may suggest that FGFR signaling in MTs or in the nephrogenic mesenchyme is essential for the maintenance of the cranial part of the WD.

In $Fgfr2^{WD\ flox/-}$ embryos, epithelial cell proliferation in the MM side of the UB did not show any significant reduction. The expression pattern of Ret, *Etv4*, and *Etv5* in $Fgfr2^{WD\ flox/-}$ embryos indicated that RTK signaling via RET was retained in the MM side of the UB. These results are consistent with the previous findings that UB outgrowth is regulated mainly by GDNF/RET signaling (Moore et al., 1996; Pichel et al., 1996; Sainio et al., 1997; Sanchez et al., 1996; Schuchardt et al., 1994). In *Ret* KO mice, almost 40% of embryos show ureteric budding, and additional inhibition of FGFR signaling completely abolishes UB formation (Michos et al., 2010; Schuchardt et al., 1994). These previous observations indicate partial redundancy between RET and FGFR signaling in the UB.

The current work demonstrated that *Ret* expression was reduced in the WD epithelia, except in the MM side of the UB in $Fgfr2^{WD\ flox/-}$ embryos, suggesting that *Fgfr2* probably regulates GDNF/RET signaling in the WD of the caudal mesonephros and the coelom side of the UB. However, analysis of *Ret* KO embryos suggests that GDNF/RET signaling is dispensable for *Etv* expression and also for cell proliferation (data not shown) in these parts. These results indicate that RTK signaling via FGFR is required for WD development.

To our knowledge, *Fgf10* is the only RTK ligand that is distinctly expressed in the mesenchyme of the caudal mesonephros and of the coelom side of the UB at E10.5. In contrast, *Gdnf* is prominently expressed in the metanephric mesenchyme. This region-specific expression pattern of RTK ligands may explain the region-specific FGFR2 dependency of RTK signaling in the WD epithelia, *i.e.*, the possible redundancy of RTK signaling between FGF and GDNF in the MM side of the UB but not in the coelom side and the WD of the caudal mesonephros.

In conclusion, the current study demonstrates that WD epithelial cell proliferation is regulated by distinct region-specific mechanisms during its development. The results suggest that FGFR signaling is essential for cell proliferation of the WD in the caudal mesonephros and the coelom side of the UB. The WD is fundamental not only for the development of the transient or definitive kidneys but also for the development of the reproductive tract. The WD is also essential for the formation of the Mullerian duct (MD), female reproductive tract anlarge. The MD extends from cranial to caudal under the guidance of the WD around E12.5 (Mullen and Behringer, 2014). Therefore, it is possible that the abnormality observed in the current mutant embryos may also consequently affect the MD development and female reproductive tract development. Further analyses regarding

female embryos may provide broad function of FGF signaling in reproductive tract formation. The current study provides novel insights into the regulation of urogenital tract development, including male and female reproductive tract, and kidney.

Supplementary Material

Refer to Web version on PubMed Central for supplementary material.

Acknowledgments

We thank Dr. Hideki Enomoto, Dr. Anne M. Moon, Dr. Chuxia Deng, Dr. Ryuichi Nishinakamura, Dr. Nobuyuki Itoh, and Dr. Hideyo Ohuchi for their supports. We also express our appreciation to Dr. Kentaro Suzuki, Dr. Daisuke Matsumaru, Dr. Akiko Omori, Dr. Lerrie A. Ipulan, Dr. Dennis D. Raga, Hiroko Suzuki, Shoko Matsushita, and Yoshitsugu Sakita for their assistance. We thank Tomiko I. Iba for technical help. This work is supported by Grant-in-Aid for Young Scientists B (25860771) and for Scientific Research on Innovative Areas: Molecular mechanisms for establishment of Sex differences (22132006). This work is also supported by National Institutes of Health Grant R01ES016597 (G. Yamada) and R01HL111190 (D. M. Ornitz).

Appendix A. Supporting information

Supplementary data associated with this article can be found in the online version at http://dx.doi.org/10.1016/j.ydbio.2015.01.023.

References

Araki K, Imaizumi T, Okuyama K, Oike Y, Yamamura K. Efficiency of recombination by Cre transient expression in embryonic stem cells: comparison of various promoters. J Biochem. 1997; 122:977–982. [PubMed: 9443813]

Atsuta Y, Tadokoro R, Saito D, Takahashi Y. Transgenesis of the Wolffian duct visualizes dynamic behavior of cells undergoing tubulogenesis *in vivo*. Dev Growth Differ. 2013; 55:579–590. [PubMed: 23550588]

Basson MA, Akbulut S, Watson-Johnson J, Simon R, Carroll TJ, Shakya R, Gross I, Martin GR, Lufkin T, McMahon AP, Wilson PD, Costantini FD, Mason IJ, Licht JD. Sprouty1 is a critical regulator of GDNF/RET-mediated kidney induction. Dev Cell. 2005; 8:229–239. [PubMed: 15691764]

Bates CM. Role of fibroblast growth factor receptor signaling in kidney development. Am J Physiol Renal Physiol. 2011; 301:F245–251. [PubMed: 21613421]

Batourina E, Gim S, Bello N, Shy M, Clagett-Dame M, Srinivas S, Costantini F, Mendelsohn C. Vitamin A controls epithelial/mesenchymal interactions through Ret expression. Nat Genet. 2001; 27:74–78. [PubMed: 11138002]

Beenken A, Mohammadi M. The FGF family: biology, pathophysiology and therapy. Nat Rev Drug Discov. 2009; 8:235–253. [PubMed: 19247306]

Benazeraf B, Pourquie O. Formation and segmentation of the vertebrate body axis. Annu Rev Cell Dev Biol. 2013; 29:1–26. [PubMed: 23808844]

Bouchard M, Souabni A, Mandler M, Neubuser A, Busslinger M. Nephric lineage specification by Pax2 and Pax8. Genes Dev. 2002; 16:2958–2970. [PubMed: 12435636]

Brent AE, Tabin CJ. FGF acts directly on the somitic tendon progenitors through the Ets transcription factors Pea3 and Erm to regulate scleraxis expression. Development. 2004; 131:3885–3896. [PubMed: 15253939]

Brophy PD, Ostrom L, Lang KM, Dressler GR. Regulation of ureteric bud outgrowth by Pax2-dependent activation of the glial derived neurotrophic factor gene. Development. 2001; 128:4747–4756. [PubMed: 11731455]

Cacalano G, Farinas I, Wang LC, Hagler K, Forgie A, Moore M, Armanini M, Phillips H, Ryan AM, Reichardt LF, Hynes M, Davies A, Rosenthal A. GFRalpha1 is an essential receptor component

for GDNF in the developing nervous system and kidney. Neuron. 1998; 21:53–62. [PubMed: 9697851]

Cancilla B, Ford-Perriss MD, Bertram JF. Expression and localization of fibroblast growth factors and fibroblast growth factor receptors in the developing rat kidney. Kidney Int. 1999; 56:2025–2039. [PubMed: 10594778]

Capel B. The battle of the sexes. Mech Dev. 2000; 92:89–103. [PubMed: 10704890]

Chi X, Michos O, Shakya R, Riccio P, Enomoto H, Licht JD, Asai N, Takahashi M, Ohgami N, Kato M, Mendelsohn C, Costantini F. Ret-dependent cell rearrangements in the Wolffian duct epithelium initiate ureteric bud morphogenesis. Dev Cell. 2009; 17:199–209. [PubMed: 19686681]

Chia I, Grote D, Marcotte M, Batourina E, Mendelsohn C, Bouchard M. Nephric duct insertion is a crucial step in urinary tract maturation that is regulated by a Gata3–Raldh2–Ret molecular network in mice. Development. 2011; 138:2089–2097. [PubMed: 21521737]

Costantini F, Shakya R. GDNF/Ret signaling and the development of the kidney. BioEssays: News Rev Mol Cell Dev Biol. 2006; 28:117–127.

Davidson A. Mouse Kidney Development. StemBook. 2009

de Graaff E, Srinivas S, Kilkenny C, D'Agati V, Mankoo BS, Costantini F, Pachnis V. Differential activities of the RET tyrosine kinase receptor isoforms during mammalian embryogenesis. Genes Dev. 2001; 15:2433–2444. [PubMed: 11562352]

Donjacour AA, Thomson AA, Cunha GR. FGF-10 plays an essential role in the growth of the fetal prostate. Dev Biol. 2003; 261:39–54. [PubMed: 12941620]

Dressler GR. The cellular basis of kidney development. Annu Rev Cell Dev Biol. 2006; 22:509–529. [PubMed: 16822174]

Dressler GR, Deutsch U, Chowdhury K, Nornes HO, Gruss P. Pax2, a new murine paired-box-containing gene and its expression in the developing excretory system. Development. 1990; 109:787–795. [PubMed: 1977574]

Dudley AT, Godin RE, Robertson EJ. Interaction between FGF and BMP signaling pathways regulates development of metanephric mesenchyme. Genes Dev. 1999; 13:1601–1613. [PubMed: 10385628]

Dyche WJ. A comparative study of the differentiation and involution of the Mullerian duct and Wolffian duct in the male and female fetal mouse. J Morphol. 1979; 162:175–209. [PubMed: 537099]

Enomoto H, Araki T, Jackman A, Heuckeroth RO, Snider WD, Johnson EM Jr, Milbrandt J. GFR alpha1-deficient mice have deficits in the enteric nervous system and kidneys. Neuron. 1998; 21:317–324. [PubMed: 9728913]

Enomoto H, Crawford PA, Gorodinsky A, Heuckeroth RO, Johnson EM Jr, Milbrandt J. RET signaling is essential for migration, axonal growth and axon guidance of developing sympathetic neurons. Development. 2001; 128:3963–3974. [PubMed: 11641220]

Finch PW, Cunha GR, Rubin JS, Wong J, Ron D. Pattern of keratinocyte growth factor and keratinocyte growth factor receptor expression during mouse fetal development suggests a role in mediating morphogenetic mesenchymal–epithelial interactions. Dev Dyn Off Publ Am Assoc Anat. 1995; 203:223–240.

Firnberg N, Neubüser A. FGF signaling regulates expression of Tbx2, Erm, Pea3, and Pax3 in the early nasal region. Dev Biol. 2002; 247:237–250. [PubMed: 12086464]

Grieshammer U, Le M, Plump AS, Wang F, Tessier-Lavigne M, Martin GR. SLIT2-mediated ROBO2 signaling restricts kidney induction to a single site. Dev Cell. 2004; 6:709–717. [PubMed: 15130495]

Hains D, Sims-Lucas S, Kish K, Saha M, McHugh K, Bates CM. Role of fibroblast growth factor receptor 2 in kidney mesenchyme. Pediatr Res. 2008; 64:592–598. [PubMed: 18670373]

Haraguchi R, Suzuki K, Murakami R, Sakai M, Kamikawa M, Kengaku M, Sekine K, Kawano H, Kato S, Ueno N, Yamada G. Molecular analysis of external genitalia formation: the role of fibroblast growth factor (Fgf) genes during genital tubercle formation. Development. 2000; 127:2471–2479. [PubMed: 10804187]

Hebert JM. FGF signaling through FGFR1 is required for olfactory bulb morphogenesis. Development. 2003; 130:1101–1111. [PubMed: 12571102]

Hinton, BT.; Lan, ZJ.; Lye, RJ.; Labus, JC. Regulation of epididymal function by testicular factors: the lumicrine hypothesis. In: Goldberg, E., editor. The Testis. Springer; New York: 2000. p. 163-173.

Hoshi M, Batourina E, Mendelsohn C, Jain S. Novel mechanisms of early upper and lower urinary tract patterning regulated by RetY1015 docking tyrosine in mice. Development. 2012; 139:2405–2415. [PubMed: 22627285]

Jain S, Encinas M, Johnson EM Jr, Milbrandt J. Critical and distinct roles for key RET tyrosine docking sites in renal development. Genes Dev. 2006; 20:321–333. [PubMed: 16452504]

Joseph A, Yao H, Hinton BT. Development and morphogenesis of the Wolffian/epididymal duct, more twists and turns. Dev Biol. 2009; 325:6–14. [PubMed: 18992735]

Kitagaki J, Ueda Y, Chi X, Sharma N, Elder CM, Truffer E, Costantini F, Lewandoski M, Perantoni AO. FGF8 is essential for formation of the ductal system in the male reproductive tract. Development. 2011; 138:5369–5378. [PubMed: 22110055]

Kobayashi A, Kwan KM, Carroll TJ, McMahon AP, Mendelsohn CL, Behringer RR. Distinct and sequential tissue-specific activities of the LIM-class homeobox gene Lim1 for tubular morphogenesis during kidney development. Development. 2005; 132:2809–2823. [PubMed: 15930111]

Kume T, Deng K, Hogan BL. Murine forkhead/winged helix genes Foxc1 (Mf1) and Foxc2 (Mfh1) are required for the early organogenesis of the kidney and urinary tract. Development. 2000; 127:1387–1395. [PubMed: 10704385]

Liu Y, Jiang H, Crawford HC, Hogan BLM. Role for ETS domain transcription factors Pea3/Erm in mouse lung development. Dev Biol. 2003; 261:10–24. [PubMed: 12941618]

Maeshima A, Sakurai H, Choi Y, Kitamura S, Vaughn DA, Tee JB, Nigam SK. Glial cell-derived neurotrophic factor independent ureteric bud outgrowth from the Wolffian duct. J Am Soc Nephrol: JASN. 2007; 18:3147–3155.

Mason IJ, Fuller-Pace F, Smith R, Dickson C. FGF-7 (keratinocyte growth factor) expression during mouse development suggests roles in myogenesis, forebrain regionalisation and epithelial-mesenchymal interactions. Mech Dev. 1994; 45:15–30. [PubMed: 8186145]

Mendelsohn C. Using mouse models to understand normal and abnormal urogenital tract development. Organogenesis. 2009; 5:306–314. [PubMed: 19568352]

Michael L, Davies JA. Pattern and regulation of cell proliferation during murine ureteric bud development. J Anat. 2004; 204:241–255. [PubMed: 15061751]

Michos O, Cebrian C, Hyink D, Grieshammer U, Williams L, D'Agati V, Licht JD, Martin GR, Costantini F. Kidney development in the absence of Gdnf and Spry1 requires Fgf10. PLoS Genet. 2010; 6:e1000809. [PubMed: 20084103]

Michos O, Panman L, Vintersten K, Beier K, Zeller R, Zuniga A. Gremlin-mediated BMP antagonism induces the epithelial–mesenchymal feedback signaling controlling metanephric kidney and limb organogenesis. Development. 2004; 131:3401–3410. [PubMed: 15201225]

Moore MW, Klein RD, Farinas I, Sauer H, Armanini M, Phillips H, Reichardt LF, Ryan AM, Carver-Moore K, Rosenthal A. Renal and neuronal abnormalities in mice lacking GDNF. Nature. 1996; 382:76–79. [PubMed: 8657308]

Mugford JW, Sipila P, McMahon JA, McMahon AP. Osr1 expression demarcates a multi-potent population of intermediate mesoderm that undergoes progressive restriction to an Osr1-dependent nephron progenitor compartment within the mammalian kidney. Dev Biol. 2008; 324:88–98. [PubMed: 18835385]

Mullen RD, Behringer RR. Molecular genetics of Mullerian duct formation, regression and differentiation. Sex Dev Genet Mol Biol Evol Endocrinol Embryol Pathol Sex Determ Differ. 2014; 8:281–296.

Murashima A, Akita H, Okazawa M, Kishigami S, Nakagata N, Nishinakamura R, Yamada G. Midline-derived Shh regulates mesonephric tubule formation through the paraxial mesoderm. Dev Biol. 2014; 386:216–226. [PubMed: 24370450]

Nishinakamura R, Matsumoto Y, Nakao K, Nakamura K, Sato A, Copeland NG, Gilbert DJ, Jenkins NA, Scully S, Lacey DL, Katsuki M, Asashima M, Yokota T. Murine homolog of SALL1 is essential for ureteric bud invasion in kidney development. Development. 2001; 128:3105–3115. [PubMed: 11688560]

Nishita M, Qiao S, Miyamoto M, Okinaka Y, Yamada M, Hashimoto R, Iijima K, Otani H, Hartmann C, Nishinakamura R, Minami Y. Role of Wnt5a-Ror2 signaling in morphogenesis of the metanephric mesenchyme during ureteric budding. Mol Cell Biol. 2014; 34:3096–3105. [PubMed: 24891614]

Ornitz DM, Itoh N. Fibroblast growth factors. Genome Biol. 2001; 2 (REVIEWS3005).

Ornitz DM, Xu J, Colvin JS, McEwen DG, MacArthur CA, Coulier F, Gao G, Goldfarb M. Receptor specificity of the fibroblast growth factor family. J Biol Chem. 1996; 271:15292–15297. [PubMed: 8663044]

Orr-Urtreger A, Givol D, Yayon A, Yarden Y, Lonai P. Developmental expression of two murine fibroblast growth factor receptors, flg and bek. Development. 1991; 113:1419–1434. [PubMed: 1667382]

Ozawa K, Uruno T, Miyakawa K, Seo M, Imamura T. Expression of the fibroblast growth factor family and their receptor family genes during mouse brain development. Brain Res Mol Brain Res. 1996; 41:279–288. [PubMed: 8883961]

Paek H, Gutin G, Hebert JM. FGF signaling is strictly required to maintain early telencephalic precursor cell survival. Development. 2009; 136:2457–2465. [PubMed: 19542358]

Peters KG, Werner S, Chen G, Williams LT. Two FGF receptor genes are differentially expressed in epithelial and mesenchymal tissues during limb formation and organogenesis in the mouse. Development. 1992; 114:233–243. [PubMed: 1315677]

Pichel JG, Shen L, Sheng HZ, Granholm AC, Drago J, Grinberg A, Lee EJ, Huang SP, Saarma M, Hoffer BJ, Sariola H, Westphal H. Defects in enteric innervation and kidney development in mice lacking GDNF. Nature. 1996; 382:73–76. [PubMed: 8657307]

Poladia DP, Kish K, Kutay B, Hains D, Kegg H, Zhao H, Bates CM. Role of fibroblast growth factor receptors 1 and 2 in the metanephric mesenchyme. Dev Biol. 2006; 291:325–339. [PubMed: 16442091]

Sainio K, Suvanto P, Davies J, Wartiovaara J, Wartiovaara K, Saarma M, Arumae U, Meng X, Lindahl M, Pachnis V, Sariola H. Glial-cell-line-derived neurotrophic factor is required for bud initiation from ureteric epithelium. Development. 1997; 124:4077–4087. [PubMed: 9374404]

Sanchez MP, Silos-Santiago I, Frisen J, He B, Lira SA, Barbacid M. Renal agenesis and the absence of enteric neurons in mice lacking GDNF. Nature. 1996; 382:70–73. [PubMed: 8657306]

Saxen, L. Organogenesis of the Kidney. Cambridge University Press; New York, USA: 1987.

Schlessinger J. Cell signaling by receptor tyrosine kinases. Cell. 2000; 103:211–225. [PubMed: 11057895]

Schuchardt A, D'Agati V, Larsson-Blomberg L, Costantini F, Pachnis V. Defects in the kidney and enteric nervous system of mice lacking the tyrosine kinase receptor Ret. Nature. 1994; 367:380–383. [PubMed: 8114940]

Schuchardt A, D'Agati V, Pachnis V, Costantini F. Renal agenesis and hypodysplasia in ret-k- mutant mice result from defects in ureteric bud development. Development. 1996; 122:1919–1929. [PubMed: 8674430]

Shakya R, Jho EH, Kotka P, Wu Z, Kholodilov N, Burke R, D'Agati V, Costantini F. The role of GDNF in patterning the excretory system. Dev Biol. 2005; 283:70–84. [PubMed: 15890330]

Shum WW, Ruan YC, Da Silva N, Breton S. Establishment of cell–cell cross talk in the epididymis: control of luminal acidification. J Androl. 2011; 32:576–586. [PubMed: 21441423]

Sims-Lucas S, Di Giovanni V, Schaefer C, Cusack B, Eswarakumar VP, Bates CM. Ureteric morphogenesis requires Fgfr1 and Fgfr2/Frs2alpha signaling in the metanephric mesenchyme. J Am Soc Nephrol. 2012; 23:607–617. [PubMed: 22282599]

Song R, El-Dahr SS, Yosypiv IV. Receptor tyrosine kinases in kidney development. J Signal Transduct. 2011; 2011:869281. [PubMed: 21637383]

Soriano P. Generalized lacZ expression with the ROSA26 Cre reporter strain. Nat Genet. 1999; 21:70–71. [PubMed: 9916792]

Srinivas S, Watanabe T, Lin CS, William CM, Tanabe Y, Jessell TM, Costantini F. Cre reporter strains produced by targeted insertion of EYFP and ECFP into the ROSA26 locus. BMC Dev Biol. 2001; 1:4. [PubMed: 11299042]

Tee JB, Choi Y, Dnyanmote A, Decambre M, Ito C, Bush KT, Nigam SK. GDNF-independent ureteric budding: role of PI3K-independent activation of AKT and FOSB/JUN/AP-1 signaling. Biol Open. 2013; 2:952–959. [PubMed: 24143282]

Tong SY, Hutson JM, Watts LM. Does testosterone diffuse down the wolffian duct during sexual differentiation? J Urol. 1996; 155:2057–2059. [PubMed: 8618334]

Walker KA, Sims-Lucas S, Di Giovanni VE, Schaefer C, Sunseri WM, Novitskaya T, de Caestecker MP, Chen F, Bates CM. Deletion of fibroblast growth factor receptor 2 from the peri-Wolffian duct stroma leads to ureteric induction abnormalities and vesicoureteral reflux. PloS One. 2013; 8:e56062. [PubMed: 23409123]

Weiss AC, Airik R, Bohnenpoll T, Greulich F, Foik A, Trowe MO, Rudat C, Costantini F, Adams RH, Kispert A. Nephric duct insertion requires EphA4/EphA7 signaling from the pericloacal mesenchyme. Development. 2014; 141:3420–3430. [PubMed: 25139858]

White AC, Xu J, Yin Y, Smith C, Schmid G, Ornitz DM. FGF9 and SHH signaling coordinate lung growth and development through regulation of distinct mesenchymal domains. Development. 2006; 133:1507–1517. [PubMed: 16540513]

Yu J, Carroll TJ, McMahon AP. Sonic hedgehog regulates proliferation and differentiation of mesenchymal cells in the mouse metanephric kidney. Development. 2002; 129:5301–5312. [PubMed: 12399320]

Yu J, McMahon AP, Valerius MT. Recent genetic studies of mouse kidney development. Curr Opin Genet Dev. 2004; 14:550–557. [PubMed: 15380247]

Yu K, Xu J, Liu Z, Sosic D, Shao J, Olson EN, Towler DA, Ornitz DM. Conditional inactivation of FGF receptor 2 reveals an essential role for FGF signaling in the regulation of osteoblast function and bone growth. Development. 2003; 130:3063–3074. [PubMed: 12756187]

Zhang X, Ibrahimi OA, Olsen SK, Umemori H, Mohammadi M, Ornitz DM. Receptor specificity of the fibroblast growth factor family. The complete mammalian FGF family. J Biol Chem. 2006; 281:15694–15700. [PubMed: 16597617]

Zhao H. Role of fibroblast growth factor receptors 1 and 2 in the ureteric bud. Dev Biol. 2004; 276:403. [PubMed: 15581874]

Zhao M, Li D, Shimazu K, Zhou YX, Lu B, Deng CX. Fibroblast growth factor receptor-1 is required for long-term potentiation, memory consolidation, and neurogenesis. Biol Psychiatry. 2007; 62:381–390. [PubMed: 17239352]

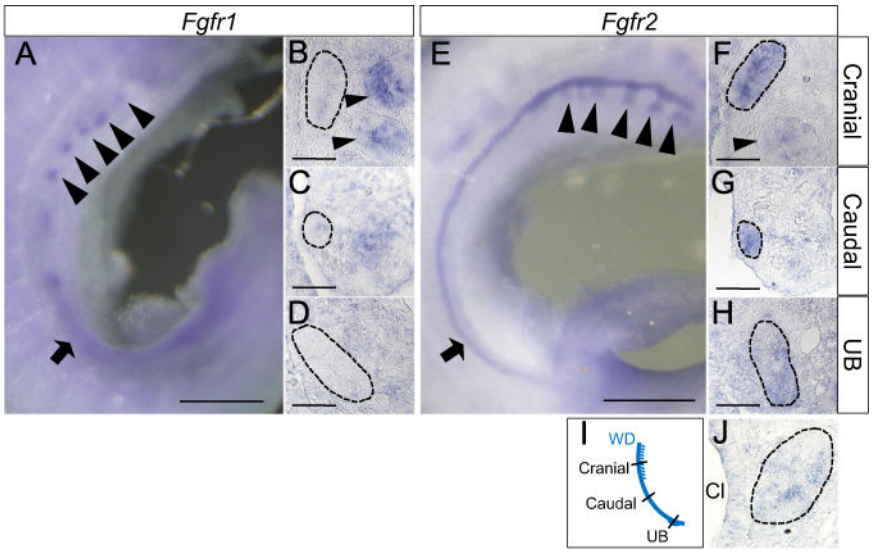

Fig. 1.

Fgfr2 is the major *Fgfr* gene expressed in the WD epithelia. Whole-mount RNA *in situ* hybridization to detect *Fgfr1* (A) and *Fgfr2* (E) expression in the mesonephros of wild-type embryos was performed at E10.5. Section RNA *in situ* hybridization to detect *Fgfr1* (B–D) and *Fgfr2* (F–H, and J) expression in the mesonephros of wild-type embryos was performed at E10.5. For the histological analyses of horizontal sections at E10.5, the WD is divided into three parts along the axis by the following definition: (1) cranial part, the WD where MTs are present; (2) caudal part, the WD of the caudal mesonephros (the WD between the cranial part and the UB); and (3) UB part, the WD where the pseudostratified epithelia is observed. A schematic representation of the cranial (B and F), caudal (C and G), and UB (D and H) parts in the WD at E10.5 are presented in I. *Fgfr2* expression in the portion that lies near the cloaca is shown in J. Scale bars: A and E, 500 μm; B–D, F–H, and J, 50 μm. Arrow, WD; arrowheads, MTs; dashed line, WD epithelia; Cl, cloaca.

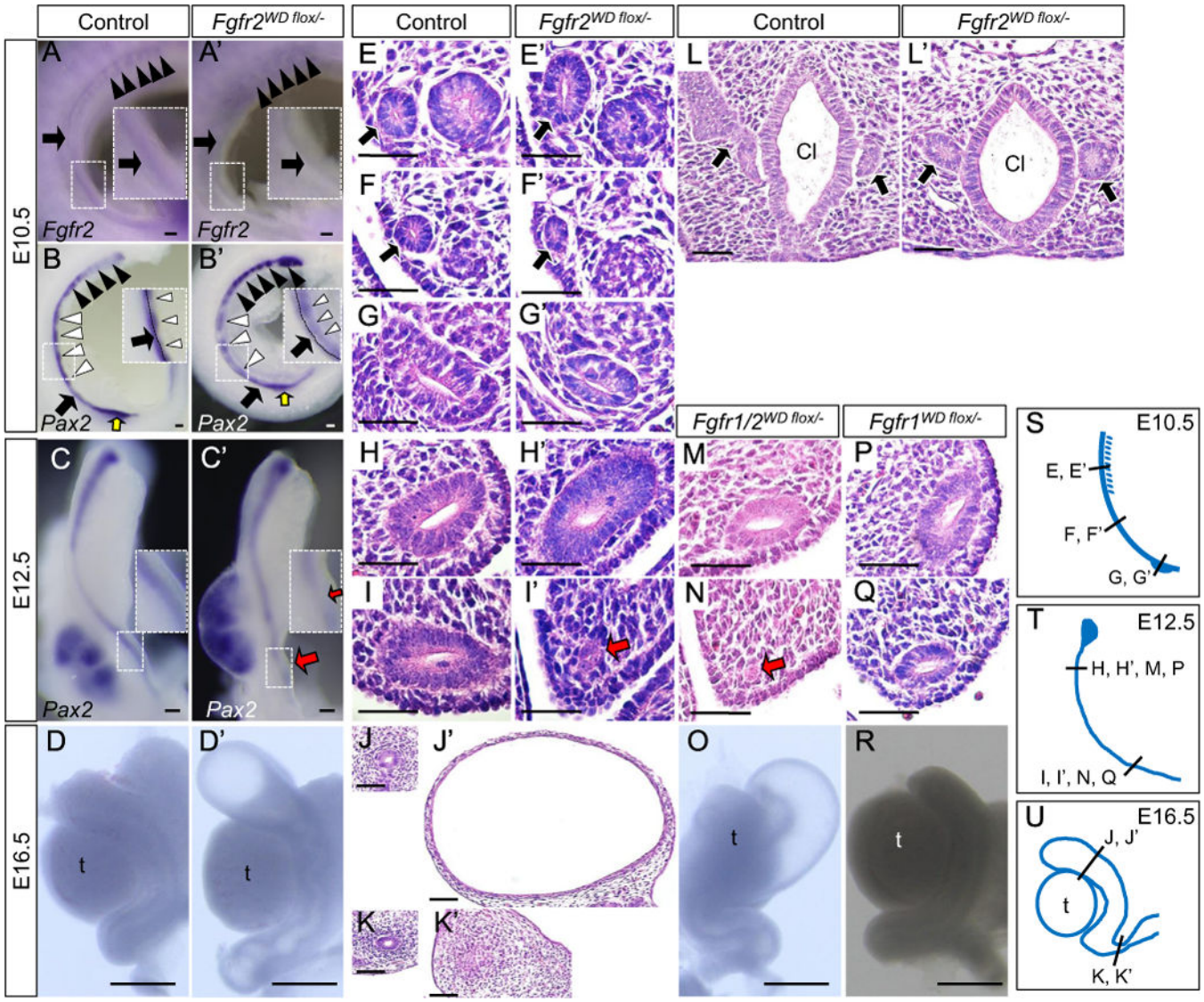

Fig. 2.

WD-specific inactivation of *Fgfr2* results in WD regression in the caudal mesonephros. Whole-mount RNA *in situ* hybridization to detect *Fgfr2* expression in the WD and MTs of the control (A) and $Fgfr2^{WD\ flox/-}$ (A′) embryos was performed at E10.5. Insets show high magnification views of the caudal mesonephros (A and A′). The WD and MTs are marked by *Pax2* expression in the control (B and C) and $Fgfr2^{WD\ flox/-}$ (B′ and C′) embryos at E10.5 (B and B′) and E12.5 (C and C′). Insets show high magnification views of the caudal mesonephros (B, B′, Cand C′). The gross morphology of the WD and testis at E16.5 is shown inD (control) and D′ ($Fgfr2^{WD\ flox/-}$). HE staining of the WD in the control (E–L) and $Fgfr2^{WD\ flox/-}$ (E′–L′) embryos was performed at E10.5 (E–G, L, E′–G′, and L′), E12.5 (H, I, H′, and I′), and E16.5 (J, K, J′, and K′). Schematic representations indicating the axial levels of the WD at E10.5, E12.5, and E16.5 are presented in S, T, and U. The WD that lies near the cloaca is shown in L (Control) and L′ ($Fgfr2^{WD\ flox/-}$). HE staining at E12.5 and the gross morphology of the WD and testis at E16.5 in $Fgfr1/2^{WD\ flox/-}$ and $Fgfr1^{WD\ flox/-}$

embryos are shown in M–O and P–R. Scale bars: A–C and A′–C′, 100 μm; D, D′, O, and R, 500 μm; E–N, P, Q, and E′–L′, 50 μm. Black arrow, WD; black arrowheads, MTs; white arrowheads, condensed mesenchyme; yellow arrow, UB; red arrow, regression of WD epithelia; Cl, cloaca; t, testis.

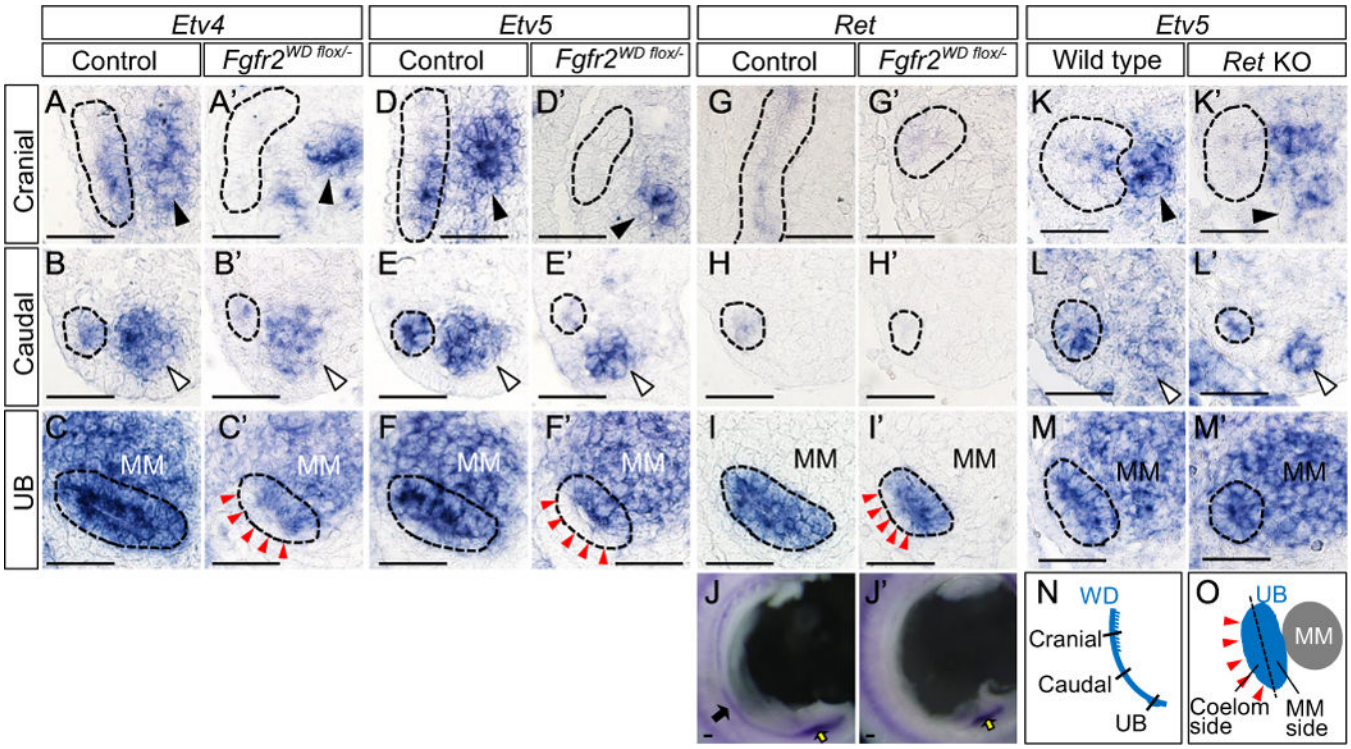

Fig. 3.

Decreased expression of the downstream target genes of RTK signaling in the WD epithelia *of Fgfr2*$^{WD\ flox/-}$ embryos. Section RNA *in situ* hybridization for *Etv4* (A–C and A′–C′), *Etv5* (D–F and D′–F′), and *Ret* (G–I and G′–I′) in E10.5 embryos in the cranial (A, A′, D, D′, G, and G′), caudal (B, B′, E, E′, H, and H′), and UB (C, C′, F, F′, I, and I′) parts was performed in the control (A–I) and *Fgfr2*$^{WD\ flox/-}$ (A′–I′) embryos. Whole-mount RNA *in situ* hybridization to detect *Ret* expression was performed in the control (J) and *Fgfr2*$^{WD\ flox/-}$ (J′) embryos at E10.5. Section RNA *in situ* hybridization for *Etv5* in wild-type (K–M) and *Ret* KO (K′–M′) embryos for the cranial (K and K′), caudal (L and L′), and UB (M and M′) parts was performed at E10.5. A schematic representation of the cranial, caudal, and UB parts in the WD at E10.5 is shown in N. A schematic representation of the MM and coelom sides of the UB at E10.5 is shown in O. Scale bars: A–I, K–M, A′–I′, and K′–M′, 50 μm; J and J′, 100 μm. Dashed line, WD epithelia; black arrowhead, MT; white arrowhead, condensed mesenchyme; MM, metanephric mesenchyme; red arrows, coelom side of the UB; yellow arrow, UB.

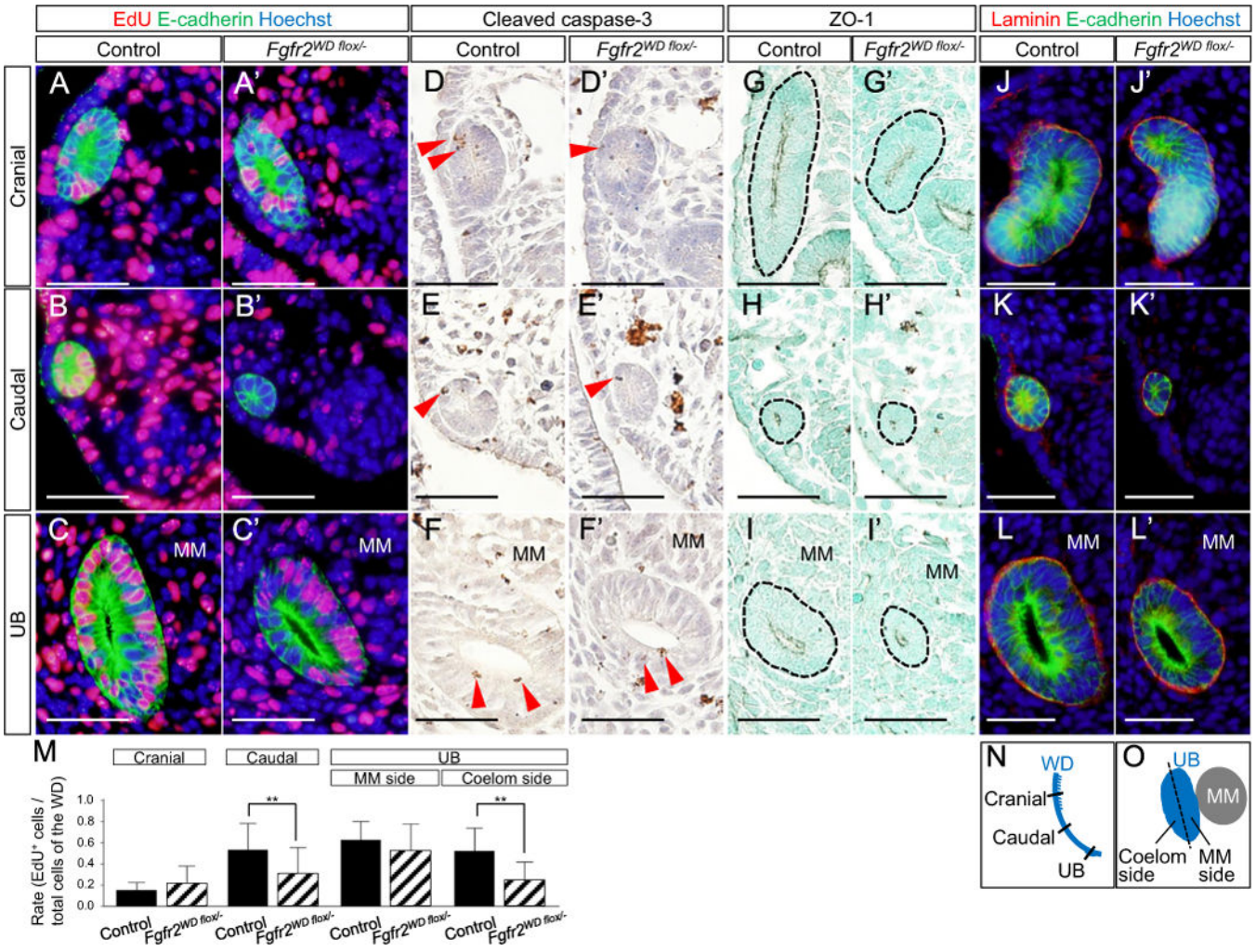

Fig. 4.

FGFR signaling regulates cell proliferation in the WD of the caudal mesonephros and the coelom side of the UB. Proliferative cells were labeled with EdU (red) and co-stained with E-cadherin (green) at the cranial (A and A′), caudal (B and B′), and UB (C and C′) parts in the control (A–C) and *Fgfr2*$^{WD\ flox/-}$ (A′–C′) embryos. Nuclei were stained with Hoechst 33342. Immunohistochemistry for cleaved caspase-3 demonstrated the presence of apoptotic cells at the axial levels of the cranial (D and D′), caudal (E and E′), and UB (F and F′) parts in the control (D–F) and *Fgfr2*$^{WD\ flox/-}$ embryos (D′–F′). Sections were counterstained with hematoxylin. Immunohistochemistry for ZO-1 was performed at the axial levels of the cranial (G and G′), caudal (H and H′), and UB (I and I′) parts in the control (G–I) and *Fgfr2*$^{WD\ flox/-}$ (G′–I′) embryos. Sections were counterstained with methyl green. Immunofluorescence staining of laminin (red) and E-cadherin (green) in sections of E10.5 WD was performed at the axial levels of the cranial (J and J′), caudal (K and K′), and UB (L and L′) parts in the control (J–L) and *Fgfr2*$^{WD\ flox/-}$ (J′–L′) embryos. Nuclei were stained with Hoechst 33342. The graph (M) demonstrated the rate of EdU-positive cells per total cells in the WD epithelia in the control and *Fgfr2*$^{WD\ flox/-}$ embryos. A schematic representation of the cranial, caudal, and UB parts in the WD at E10.5 is presented in N. The

UB is divided into two domains, the MM side and coelom side, as indicated in O. Scale bars: 50 μm. Red arrowheads, signals of cleaved caspase-3; dashed line, WD epithelia; MM, metanephric mesenchyme.

**$P < 0.01$; n = 4 per genotype (cranial and caudal), n = 6 per genotype (UB); values are mean + SD.

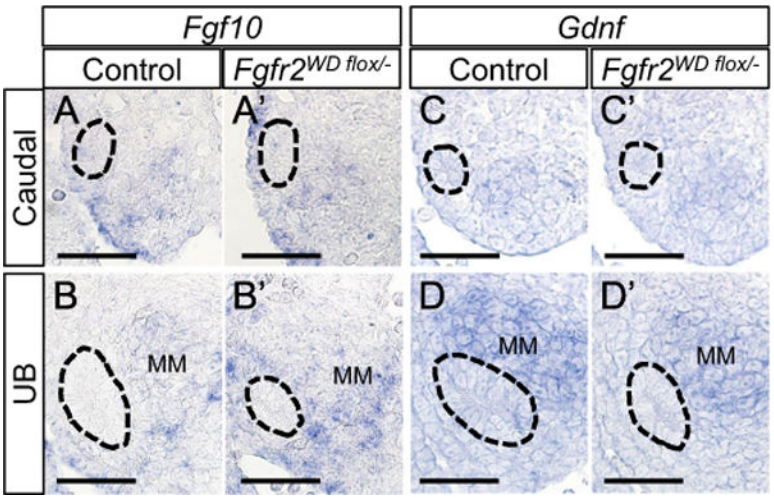

Fig. 5.

Region-specific distribution of RTK ligands in the mesonephros and metanephros. Section RNA *in situ* hybridization for *Fgf10* (A, A′, B, and B′) and *Gdnf* (C, C′, D, and D′) in the caudal mesonephros (A, A′, C, and C′) and UB (B, B′, D, and D′) was performed in the control (A–D) and $Fgfr2^{WD\ flox/-}$ (A′–D′) embryos at E10.5. Scale bars: 50 μm. Dashed line, WD epithelia; MM, metanephric mesenchyme.

Table 1

Phenotypic incidence of *Fgfr2*$^{WD\ flox/-}$, *Fgfr1/2*$^{WD\ flox/-}$ and *Fgfr*1$^{WD\ flox/-}$ embryos.

Individual allele with genotype	E12.5	E16.5
Hoxb7-Cre; Fgfr1$^{flox/+}$*; Fgfr2*$^{flox/-}$ (*Fgfr2*$^{WD\ flox/-}$)	8/10	4/6
Hoxb7-Cre; Fgfr1$^{flox/-}$; *Fgfr2*$^{flox-}$ (*Fgfr1/2*$^{WD\ flox/-}$)	3/3	2/3
Hoxb7-Cre; Fgfr1$^{flox/-}$; *Fgfr2*$^{flox/+}$ (*Fgfr1*$^{WD\ flox/-}$)	0/8	0/4